A Multifilament Method-of-Moments Solution for the Input Impedance of a Probe-Excited Semi-Infinite Waveguide

JOHN M. JAREM, MEMBER, IEEE

Abstract — **The input impedance and surface currents of a probe-excited, short-circuited semi-infinite waveguide are determined by the method of moments. Expressions are given for the impressed electric field used to excite the probe from the coaxial source input using a semi-infinite-waveguide Green's function, and expressions are given for a free-space approximate impressed electric field which arises from the coaxial source input. The method-of-moments formulation used is based on a multifilament current approximation and solves for the surface currents of the probe as a function of probe angle around the probe. Comparison of theory and experiment is made.**

I. Introduction

AN IMPORTANT PROBLEM in microwave theory is the problem of determining the input impedance of a coaxial probe when it is inserted into a waveguide which is short circuited on one side and extends to infinity on the other. This problem of determining the input impedance has been studied by Collin [1], and the closely related problem of determining the input impedance of a coaxial feed into a rectangular waveguide which is infinite on both sides has been studied by Al-Hakkak [2], Williamson [3]–[8], and others.

In the studies of Collin [1] and Al-Hakkak [2], the impedance analysis consists of determining a Green's function for the EM fields and currents in a semi-infinite rectangular waveguide and then extremalizing a variational impedance expression which is based on the above Green's function to determine the input impedance of the probe in the waveguide system. In the analysis of [1], [2], a single modal current was used as a trial function. In the studies of Williamson [3]–[8], the problem of determining the input impedance of a probe in an infinite rectangular waveguide was analyzed by using a method-of-moments technique [3], [4] and was analyzed by deriving a closed-form impedance expression [5]–[8]. The above techniques of Williamson [3]–[8] were based on defining and using an appropriate set of Green's functions to describe the fields and currents in the waveguide.

An important assumption that was made in both the studies of [1], [2] and [3]–[8] was that the electric current which flowed on the probe surface was uniform in distribution around the probe. Two important further assumptions that were made by [1], [2] were that this current could be effectively represented by a filamentary current located at the center of the probe and that the impressed electric field which radiates from the coaxial base was extremely localized at the base of the probe and could be treated as such.

At this point, it is useful to discuss these assumptions in relation to the exact probe waveguide problem which actually occurs and in relation to a multifilament method-of-moments analysis made by Leviatan *et al.* [9], [10]. Concerning the first two assumptions, a recent analysis by Leviatan *et al.* [9], [10], which concerned the scattering of a TE_{10} mode from a top-to-bottom cyclindrical post in a rectangular waveguide, showed that even for posts with relatively thin radii the probe's surface current was nonuniform in angle around the probe. This analysis also showed that the nonuniform currents of larger posts had more effect on the scattering parameters of the post systems than did smaller ones. Based on the above investigations [9], [10], a natural question that arises is whether the probe current in the present problem is significantly nonuniform. Concerning the assumption about the impressed source electric field, to the author's knowledge no analysis has studied how the impressed electric field, given by an exact semi-infinite-waveguide Green's function, that occurs at the base of a coaxial probe affects the input impedance of the overall system.

In the light of the above discussion, the purpose of this paper will be to solve for the input impedance of a coaxial probe in a semi-infinite waveguide using a method-of-moments formulation based on a nonuniform surface current approximation and on the use of an impressed electric field arising from a semi-infinite-waveguide Green's function.

II. Method-of-Moments Equations

This section will be concerned with presenting the electric-field integral equations, Green's functions, and matrix equations which can be used to solve for the input impedance of a coaxial probe in a semi-infinite waveguide for the geometry shown in Fig. 1.

In this analysis, it will be assumed that the probe is

Manuscript received April 10, 1986; revised July 7, 1986. This work was supported in part by a research contract (Document Number 95-1400) from Antenna Development (2343), Sandia National Laboratories Albuquerque, NM.

The author is with the University of Texas at El Paso, El Paso, TX 79968.

IEEE Log Number 8611022.

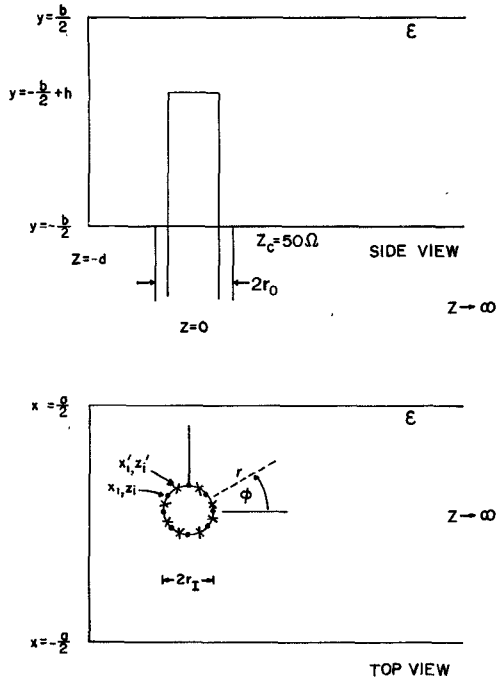

Fig. 1. The geometry of the semi-infinite rectangular waveguide under consideration is shown. The x's and dots shown in the lower figure (top view) represent the location of the filamentary current source points (x) and electric-field testing points (dots).

centered in the waveguide and that a set of eight filamentary currents, shown in Fig. 1, represent the surface current on the probe surface. Symmetry of the probe position shows that only four of the eight filamentary currents need to be solved for. It will also be assumed that each filamentary current, which represents a 45° slice of the probe surface current, can be represented as an expansion of modal functions which vary with vertical position on the probe (the y coordinate of Fig. 1).

The basic electromagnetic boundary condition in this problem is the boundary condition that the total E_{yT} electric field at the probe surface equals zero. The total electric field at a point on the probe surface is composed of terms which are due to radiation from each 45° filamentary current making up the probe current and to radiation from the coaxial frill source at the base of the probe. In this analysis, the electric-field boundary condition will be imposed by setting the electric field to zero at the dot points shown in Fig. 1. These points have been chosen because they provide a maximum separation between the testing points on the probe and the source points on the probe and, as later calculations will show, thereby provide spacing which will allow the most rapid convergence possible of the Green's functions of the system.

Mathematically, the probe electric-field equation is given by

$$\sum_{i'=1}^{8} E^J_{yi,i'} + E^I_{yi} = 0, \qquad i = 1, \cdots, 4 \tag{1}$$

where $E^J_{yi,i'}$ represents the radiation from the i' filamentary source to electric-field point i, and E^I_{yi} represents the electric field which radiates from the frill source at the probe base to the point where the electric field is being evaluated. The coordinates of the i' and i points in Fig. 1 are given by

$$x'_{i'} = r_I \sin\phi'_{i'}, \qquad z'_{i'} = r_I \cos\phi'_{i'} \tag{2}$$

$$x_i = r_I \sin\phi_i, \qquad z_i = r_I \cos\phi_i \tag{3}$$

$$\phi'_{i'} = \left(i' - \tfrac{1}{2}\right)\Delta\phi \qquad i' = 1, \cdots, 8$$

$$\phi_i = (i-1)\,\Delta\phi \qquad i = 1, \cdots, 4$$

$$\Delta\phi = \pi/4.$$

The $E^J_{yi,i'}$ electric field is given by

$$E^J_{yi,i'} = r_I \Delta\phi \int_{-b/2}^{-b/2+h} G_{yy}(x_i, y, z_i | x'_{i'}, y', z'_{i'}) \cdot J_y(y', \phi'_{i'})\, dy' \tag{4}$$

where

$$J_y(y', \phi') = \sum_{s'=1}^{2} j_{s'i'} t_{s'}(y')\, p_{i'}(\phi') \tag{5}$$

$$t_{s'}(y) = \begin{cases} \sin k\left(h - \left(y + \dfrac{b}{2}\right)\right) & s' = 1 \\ t_1(y) + \alpha\left[1 - \cos k\left(h - \left(y + \dfrac{b}{2}\right)\right)\right] & s' = 2 \end{cases}$$

$$p_{i'}(\phi') = \begin{cases} 1 & \phi'_{i'} - \dfrac{\Delta}{2} < \phi' < \phi'_{i'} + \dfrac{\Delta}{2} \\ 0 & \text{elsewhere} \end{cases} \tag{6}$$

where

$$\alpha = -\int_{-b/2}^{-b/2+h} t_1^2(y)\, dy \Big/ \int_{-b/2}^{-b/2+h} t_1(y)\left[1 - \cos k\left(h - \left(y + \frac{b}{2}\right)\right)\right] dy.$$

In (4) and (5), $j_{s'i'}$ (A/cm) represents a set of multifilament coefficients which are used to expand the unknown surface current J_y; G_{yy} represents the yy component of a semi-infinite rectangular waveguide dyadic Green's function. The coefficients $j_{s'i'}$ have been called multifilament expansion coefficients because of the way G_{yy} and J_y in (4) were point sampled in ϕ' and thus behaved as if they were multifilament sources.

The constant α in (6) has been chosen so that t_1 and t_2 are orthogonal with weight 1 to one another in the interval $0 \leqslant y + b/2 \leqslant h$. This ensures that t_1 and t_2 form a linearly independent set and thus are suitable as expansion functions.

The Green's function in (4) is given by

$$G_{yy} = -\frac{2j\eta}{kab} \sum_{n=0}^{\infty} \frac{\left(-k_y^2 + k^2\right)}{\bar{\epsilon}_n} \cos k_y\left(y + \frac{b}{2}\right) \cdot \cos k_y\left(y' + \frac{b}{2}\right) \cdot \left[S_n^s(x_i, x'_{i'}, |z_i - z'_{i'}|) - S_n^s(x_i, x'_{i'}, z_i + z'_{i'} + 2d)\right] \tag{7}$$

where

$$\eta = (\mu/\epsilon)^{1/2}$$

$$S_n^s(x,x',w) = F_n^s(x,x',w) + \sum_{m=1}^{\infty} \sin k_x\left(x+\frac{a}{2}\right)\sin k_x\left(x'+\frac{a}{2}\right)\left[\frac{e^{-\gamma w}}{\gamma} - \frac{e^{-(k_x^2+k_y^2)^{1/2}w}}{\left(k_x^2+k_y^2\right)^{1/2}}\right] \tag{8}$$

$$F_n^s(x,x',w) = \begin{cases} \dfrac{a}{2\pi}\operatorname{Re}\ln\left\{\dfrac{1-T_+}{1-T_-}\right\}, & n=0 \\ \dfrac{a}{2\pi}\displaystyle\sum_{m=-\infty}^{\infty}\left[K_0\left\{k_y\left[w^2+m_-^2\right]^{1/2}\right\} - K_0\left\{k_y\left[w^2+m_+^2\right]^{1/2}\right\}\right], & n\geq 1 \end{cases} \tag{9}$$

$$T\pm = \exp\left(j\frac{\pi}{a}(|x\pm|+j|w|)\right)$$

$$m_- = 2am + x_-$$

$$m_+ = 2am + x_+$$

$$x_- = x - x'$$

$$x_+ = x + x' + a$$

$$\gamma = \begin{cases} j\left(k^2-k_x^2-k_y^2\right)^{1/2}, & k_x^2+k_y^2 < k^2 \\ \left(k_x^2+k_y^2-k^2\right)^{1/2}, & k_x^2+k_y^2 > k^2 \end{cases}$$

$$k_y = \frac{n\pi}{b}, \quad k_x = \frac{m\pi}{a}$$

K_0 = modified Bessel function of the 2nd kind

$$\bar{\epsilon}_n = \begin{cases} 2 & n=0 \\ 1 & n\neq 0 \end{cases} \tag{10}$$

and the other terms have been defined previously. As can be seen in (7), maximum convergence of the first S_n^s term of the Green's function G_{yy} occurs for maximum separation of the source and observation points. In (7), the second S_n^s term represents the interaction of the probe with its short-circuit image. In (9), the upper portion of the F_n^s term has been obtained from [9] and the lower portion from [1].

The impressed electric field E_{yi}^I, which is used in (1), has in this paper been derived by using two different methods. In the first method, the impressed electric field has been derived by using a Green's function that ignores the waveguide environment and describes only the coaxial aperture–probe surface radiation interaction. This is the Green's function which would be used to describe how a coaxial aperture radiates onto a probe in a free-space infinite ground plane system. In the second method, the impressed electric field has been obtained first by deriving the Green's function which represents how a magnetic current radiates in a semi-infinite waveguide and then by using this Green's function to find how the coaxial magnetic surface currents radiate onto the probe. The second method for determining impressed electric field requires more computational time than the first but produces more accurate results. Both methods give nearly the same impressed electric field when the probe radius is small but show significant differences as the size of the probe radius increases. The electric field E_y^I which results from the first method is given by [11]

$$E_y^I(x,y,z) = \frac{1}{2\pi}\int_0^{2\pi}\int_{r_I}^{r_0}\frac{e^{-jkr_s}}{r_s^3}[1+jkr_s] \cdot[(z-z')M_x - (x-x')M_z]r'dr'd\phi' \tag{11}$$

where

$$M_x = -\frac{E_0}{r'}\cos\phi'$$

$$M_z = \frac{E_0}{r'}\sin\phi'$$

$$E_0 = \frac{V_0}{\ln\left(\dfrac{r_0}{r_I}\right)}$$

V_0 = coaxial input voltage at $y = -\dfrac{b}{2}$

$$r_s = \left[(x-x')^2+(y-y')^2+(z-z')^2\right]^{1/2}.$$

The impressed electric field of the second, more exact method is given by

$$E_{yi}^I = \sum_{n=0}^{\infty} E_{yn}^I(x_i,z_i)\cos k_y\left(y+\frac{b}{2}\right) \tag{12}$$

where

$$E_{yn}^I = \int_0^{2\pi}\int_{r_I}^{r_0}[g_{xn}M_x + g_{zn}M_z]r'dr'd\phi' \tag{13}$$

and where M_x and M_z are given above in (11). In (12), g_{xn} and g_{zn} are the n coefficients of the Green's functions which are associated with the delta magnetic surface currents $\vec{M} = M_0\,\delta(\vec{r}-\vec{r}')\hat{a}_x$ and $\vec{M} = M_0\,\delta(\vec{r}-\vec{r}')\hat{a}_z$. Mathematically, g_{xn} and g_{zn} have been derived by the same method as was used by Collin for G_{yy} but for magnetic-type sources M_x and M_z. The g_{xn} and g_{zn} are given by

$$g_{xn}(x,z|x',z') = \frac{-2}{ab\bar{\epsilon}_n}\left[\left.\frac{\partial S_n^s}{\partial w}\right|_{w=|z-z'|}\left(\frac{z-z'}{|z-z'|}\right) + \left.\frac{\partial S_n^s}{\partial w}\right|_{w=z+z'+2d}\right] \tag{14}$$

and

$$g_{zn}(x,z|x',z') = \frac{2}{ab\bar{\epsilon}_n}\left[\left.\frac{\partial S_n^c}{\partial x}\right|_{w=|z-z'|} - \left.\frac{\partial S_n^c}{\partial x}\right|_{w=z+z'+2d}\right] \quad (15)$$

where S_n^s has been defined previously and

$$S_n^c(x,x',w) = F_n^c(x,x',w) + \sum_{m=1}^{\infty} \cos k_x\left(x+\frac{a}{2}\right) \cdot \cos k_x\left(x'+\frac{a}{2}\right)\left[\frac{e^{-\gamma w}}{\gamma} - \frac{e^{-(k_x^2+k_y^2)^{1/2}w}}{\left(k_x^2+k_y^2\right)^{1/2}}\right] \quad (16)$$

where

$$F_n^c(x,x',w) = \begin{cases} -\dfrac{a}{2\pi}\operatorname{Re}\ln\left[(1-T_+)(1-T_-)\right], & n=0 \\ -\dfrac{1}{2k_y}e^{-k_y w} + \dfrac{a}{2\pi}\displaystyle\sum_{m=-\infty}^{\infty}\left[K_0\left\{k_y\left(w^2+m_-^2\right)^{1/2}\right\} + K_0\left\{k_y\left(w^2+m_+^2\right)^{1/2}\right\}\right], & n\geq 1 \end{cases} \quad (17)$$

and the other terms have been derived previously. The upper portion of the F_n^c term has been derived by using a small modification of the analysis of [9] and the lower portion by making a small modification of Collin's analysis [1].

Once the electric field due to radiation from the probe back onto itself has been defined and the impressed electric field due to the coaxial aperture has been defined, the next step in the analysis is to convert (1) into a matrix equation which can thus be solved to find the surface currents j_{si}. This is accomplished by multiplying (1) by suitable testing functions and integrating from $-b/2$ to $-b/2+h$. The resulting equation after integration is the matrix equation

$$\sum_{i'=1}^{4}\sum_{s'=1}^{2} Z_{si,s'i'}j_{s'i'} = -\int_{-b/2}^{-b/2+h} t_s(y)E_{y_i}^I(y)\,dy = V_{si} \quad (18)$$

or

$$\underline{\underline{Z}}\,\underline{j} = \underline{V} \quad (19)$$

where $\underline{\underline{Z}}$ is determined after substitution of (4) in (1) and the integrations of the appropriate integrals have been carried out. In (18), the $t_s(y)$ of (6) was used as a testing function. Although many testing functions are possible, this one was chosen because 1) it becomes small near the probe end, as does the impressed electric field, 2) it produces a symmetric matrix equation that can be more numerically stable to invert than a nonsymmetric matrix equation which would result from other testing functions, and 3) it reduces computer time since the same function is used as an expansion function and a testing function.

Once the matrix equation is solved, the input impedance may be determined approximately from

$$z_{\text{IN}} = \frac{V_0}{\displaystyle\int_0^{2\pi} J_y\left(-\frac{b}{2},\phi\right) r_I\,d\phi} = \frac{V_0}{I_{\text{IN}}}. \quad (20)$$

A more accurate expression for input impedance can be obtained from the expressions in [7] and [12], which involve integrals over the coaxial aperture. These expressions were not derived since fairly good agreement with experiment was obtained by the use of (20). The solution of the matrix equation also provides the surface currents, scattering parameters, and power which has been radiated by the probe.

In concluding this section, we note that the formulation which has been presented can be easily modified to determine solutions for the probe current and the input impedance of the antenna system under the assumption that the probe current radiates from inside the probe surface and also under the assumption that the probe surface current is uniform. The solution which assumes that the probe surface current radiates from within the probe surface is obtained from the above formulation by replacing r_I in (2) with r_I', where $0 \leq r_I' < r_I$. This method has proved useful, as shown in [10], of producing more physical probe current solutions than when the probe current is taken to radiate from the probe surface. In the limiting case of $r_I' = 0$, the solution reduces to the center-located single-filament approximation used by Collin [1]. The uniform surface current solution, which applies when the surface current is on the probe surface $r_{I'} = r_I$ or assumed to be inside the probe surface $(0 < r_I' < r_I)$, is determined directly from the probe matrix equation by setting all of the surface current expansion coefficients $j_{s'i'}$ equal to one another for a given s' $(s' = 1,2)$, averaging the resulting set of equations over i for a given s $(s = 1,2)$, and then solving the reduced matrix equation (2×2) to determine the uniform surface current expansion coefficients. The present author recommends that, in the case when the probe radius becomes relatively large, both the above solutions be obtained in order to cross-check the solution given by (19).

III. Numerical Results

In this paper, the matrix equation, (19), was inverted for a fairly large number of different cases corresponding to different probe heights, short-circuit distances, and frequencies. In calculating these inverses, it was found that the matrix condition number ranged from relatively low

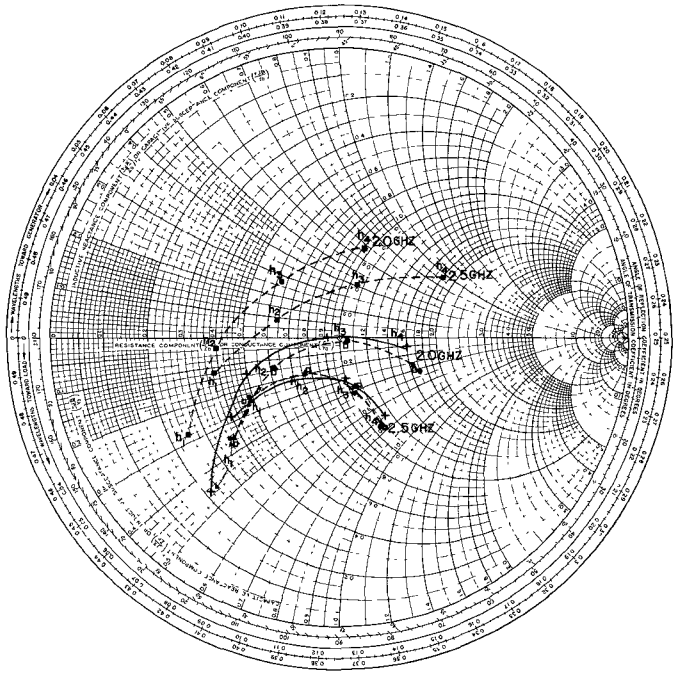

Fig. 2. The normalized input impedance as determined by Collin [1] (square), moment method with $r_I' = r_I$ (dot), uniform current approximation with $r_I' = r_I$ (solid triangle), uniform filamentary current approximation with $r_I' = 0.01\ r_I$ (hollow square) and experiment (plus) are shown for two different frequencies and four different probe heights (see text) at a radius of $r_I = 0.1778$ cm. $z_C = 50\ \Omega$ and $\bar{z}_{IN} = z_{IN}/z_C$.

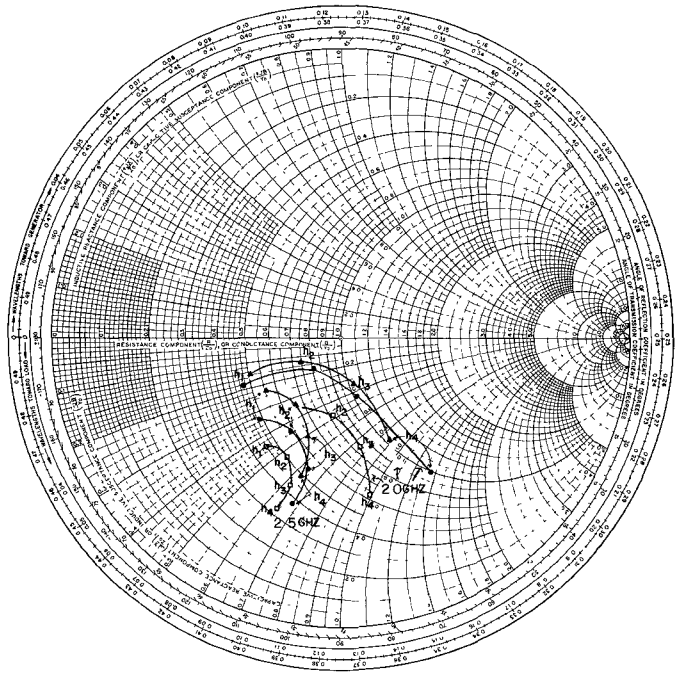

Fig. 3. The normalized input impedance as determined by moment method with $r_I' = r_I$ (dot), uniform current approximation $r_I' = r_I$ (solid triangle), and uniform filamentary current approximation $r_I' = 0.01\ r_I$ (hollow square) is shown for two different frequencies and four different probe heights (see text) at a radius of $r_I = 0.5334$ cm. $z_C = 50\ \Omega$ and $\bar{z}_{IN} = z_{IN}/z_C$.

values of 15 to high values of 500. Because of this, the matrix inversion was calculated by using the pseudoinverse method described in [13]. This method proved to be useful for the present problem because it provided the exact matrix equation solution in the cases where the condition number was low and provided low-norm, least-square error, approximate matrix solutions when the condition number was high.

A comparison of the input impedance obtained by the solution of (19) with experiment is shown in Fig. 2 for the frequencies of 2.0 GHz and 2.5 GHz and is shown when $\epsilon_R = 3.75$, $a = 5.715$ cm, $b = 2.223$ cm, $d = 1.524$ cm, $r_I = 0.1778$ cm, $h_1 = 1.270$ cm, $h_2 = 1.524$ cm, $h_3 = 1.778$ cm, and $h_4 = 2.032$ cm. Experimentally, the semi-infinite nature of the waveguide was implemented by 1) placing two probes in a variable length cavity, 2) measuring the two-port parameters of these probes at different cavity lengths, and 3) analyzing this two-port data to determine the equivalent two-port parameters of a probe which is located in a semi-infinite waveguide. Theoretically, the impedance solution shown in Fig. 2 was obtained by solving (19) using the impressed electric field given in (11) and using the pseudoinverse method. As can be seen, fairly close agreement exists between theory and experiment.

Also shown in Fig. 2 is the input impedance determined by the uniform current approximation when the probe current was assumed to be on the probe surface ($r_I' = r_I$) and when the probe was nearly center located ($r_I' = 0.01\ r_I$). As can be seen, virtually no difference in the impedance answers occurred for this radius size of $r_I = 0.1778$ cm. In contrast Collin's solution, which is based on keeping only the $t_1(y)$ term of (6), shows a very significant difference when theory and experiment are compared. The $t_2(y)$ term, when included in the analysis, greatly improves the accuracy of the analysis when compared with experiment.

Fig. 3 shows a comparison of the matrix solution (19) when $r_I' = r_I$, the uniform current approximation when $r_I' = r_I$, and the uniform current approximation when $r_I' = 0.01\ r_I$ in the case when $r_I = 0.5334$ cm and all other parameters are the same as in Fig. 2. Equation (11) was used to describe the impressed electric field. The radius value is three times that which was used in Fig. 2; thus, this case may be classified as a wide-radius case. In contrast to the impedance data of Fig. 2 ($r_I = 0.1778$ cm), the impedance data of Fig. 3 show a significant variation in impedance results when using the matrix solution, uniform current approximation ($r_I' = r_I$), and center-located filament approximation ($r_I' = 0.01\ r_I$). It is also interesting that the matrix solution shown in Fig. 3 tended to be bounded on either side by the probe surface uniform current approximation ($r_I' = r_I$) and the filamentary uniform current approximation ($r_I' = 0.01\ r_I$). Impedance calculations were made for the $r_I = 0.3556$-cm case, and similar results to Fig. 3, but with less separation, were observed.

In Fig. 4, the magnitude of the surface current is shown as a function of ϕ and of the normalized probe height coordinate $y_n = (y + b/2)/h$ for the case of $f = 2.5$ GHz, $r_I = 0.1778$ cm, $h = 1.778$ cm, and all of the other parame-

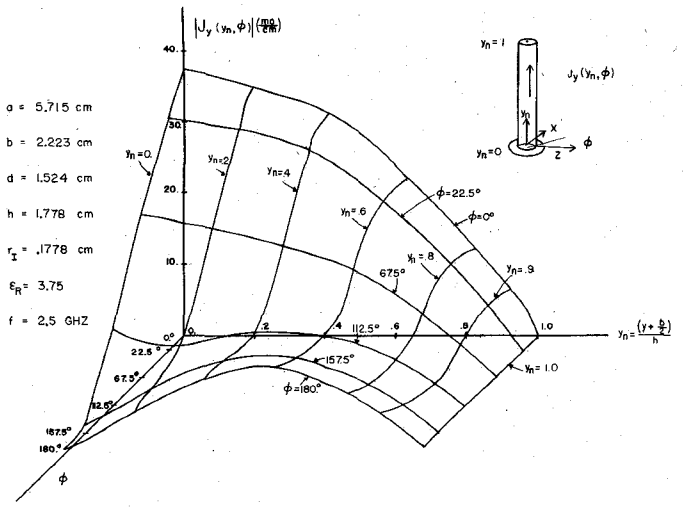

Fig. 4. The magnitude of the probe surface current (vertical axis) is shown as a function of the normalized probe height y_n (horizontal axis) and the probe angle ϕ (the third remaining axis). The ϕ indexed lines running left to right show the surface current as a function of height for a given ϕ, and the y_n indexed lines show the surface current as it varies with ϕ for a given y.

ters the same as in Fig. 2. As can be seen, a large variation in the surface current occurs around the probe.

In concluding this section, the author would like to present some general information which has been obtained by solving different cases but which has not been presented graphically. The first pieces of general information are that 1) the probe surface current determined by (19) varies greatly with angle around the probe and 2) this angular variation of the probe surface current made little difference in the input impedance except as the probe radius became large. The fact that the probe current solution varies with angle around the probe is not surprising considering the nonsymmetric waveguide environment which surrounds the probe. A second piece of information that was obtained from solving different cases was the fact that the impressed electric fields given by (11) and (13) were nearly identical when the probe radius was thin but became significantly different as the probe radius became increasingly larger. The two impressed electric-field approximations gave nearly the same impedance results for Fig. 2 but significantly different results for Fig. 3. A third result that was obtained from studying many different cases over a wide frequency range was the fact that the power delivered at the coaxial aperture equaled the power transmitted down the waveguide to within a few percent. This power conservation was observed when only a TE_{10} mode propagated and was also observed when the frequency was large enough for multimodes to propagate. Power conservation was observed to hold less well, however, as the frequency became larger or the probe radius became larger.

IV. Conclusions

A method-of-moments solution for the input impedance and probe surface currents of a probe feeding into a semi-infinite rectangular waveguide has been presented. Accurate and approximate formulas for the impressed coaxial electric field were derived. The matrix solution for the input impedance was shown to give better results for the input impedance than Collin's formulas [1]. The probe surface current was shown to vary significantly with probe angle. Overall, fairly good agreement between theory and experiment was found for the experimental cases which were tried.

Acknowledgment

The author would like to thank W. Schaedla and B. Brock for their advice and support of the present communication. He would also like to thank Antenna Development (2343) of Sandia National Laboratories, and G. Schnetzer in particular, for supplying the experimental impedance data shown in Fig. 2.

References

[1] R. E. Collin, *Field Theory of Guided Waves*. New York: McGraw-Hill, 1960, pp. 258–271.
[2] M. J. Al-Hakkak, "Experimental investigation of the input-impedance characteristics of an antenna in a rectangular waveguide," *Electron. Lett.*, vol. 5, no. 21, pp. 513–514, Oct. 16, 1969.
[3] A. G. Williamson and D. V. Otto, "Coaxially fed hollow cylindrical monopole in a rectangular waveguide," *Electron. Lett.*, vol. 9, no. 10, pp. 218–220, May 17, 1973.
[4] A. G. Williamson, "Coaxially fed hollow probe in a rectangular waveguide," *Proc. Inst. Elec. Eng.*, vol. 132, Part H, pp. 273–285, 1985.
[5] A. G. Williamson and D. V. Otto, "Cylindrical antenna in a rectangular waveguide driven from a coaxial line," *Electron. Lett.*, vol. 8, no. 22, pp. 545–547, Nov. 2, 1972.
[6] A. G. Williamson, "Equivalent circuit for a radial-line/coaxial-line junction," *Electron. Lett.*, vol. 17, no. 8, pp. 300–301, Apr. 16, 1981.
[7] A. G. Williamson, "Analysis and modelling of a coaxial-line/rectangular-waveguide junction," *Proc. Inst. Elec. Eng.*, vol. 129, Pt. H, no. 5, pp. 262–270, Oct. 1982.
[8] A. G. Williamson, "Radial line/coaxial-line junctions: Analysis and equivalent circuits," *Int. J. Electron.*, vol. 58, pp. 91–104, 1985.
[9] Y. Leviatan, P. G. Li, A. T. Adams, and J. Perini, "Single-post inductive obstacle in a rectangular waveguide," *IEEE Trans. Microwave Theory Tech.*, vol. MTT-31, pp. 806–812, Oct. 1983.
[10] Y. Leviatan, D. Shau, and A. T. Adams, "Numerical study of the current distribution on a post in a rectangular waveguide," *IEEE Trans. Microwave Theory Tech.*, vol. MTT-32, pp. 1411–1415, Oct. 1984.
[11] R. F. Harrington, *Time-Harmonic Electromagnetic Fields*. New York: McGraw-Hill, 1961.
[12] D. V. Otto, "The admittance of cylindrical antennas driven from a coaxial line," *Radio Sci.*, vol. 2 (New Series), pp. 1031–1042, Sept. 1967.
[13] M. M. Ney, "Method of moments as applied to electromagnetic problems," *IEEE Trans. Microwave Theory Tech.*, vol. MTT-33, Oct. 1985.

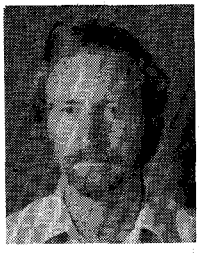

John M. Jarem (M'82) was born in Monterey, CA, on May 10, 1948. He received the B.S., M.S. and Ph.D. degrees in electrical engineering in 1971, 1972, and 1975, respectively, from Drexel University, Philadelphia, PA.

From 1975–1981, he worked as an Assistant Professor of Electrical Engineering at the University of Petroleum and Minerals, Dhahran, Saudi Arabia. He has worked for the University of Texas at El Paso as an Associate Professor of Electrical Engineering since 1981. His research interests are infrared band modeling, electromagnetics, and antenna theory.